Theoretical Study of HCN and HNC Neutral and Charged Clusters

Marina Sánchez,* Patricio F. Provasi, and Gustavo A. Aucar

Department of Physics, Northeastern University, Av. Libertad 5500, W 3404 AAS-Corrientes, Argentina

Ibon Alkorta* and Jose Elguero

Instituto de Química Médica (C.S.I.C.), Juan de la Cierva 3, 28006-Madrid, Spain

Received: June 2, 2005; In Final Form: July 8, 2005

A theoretical study of linear and cyclic clusters of $(HCN)_n$ and $(HNC)_n$ (up to $n = 10$) has been carried out by means of DFT and MP2 ab initio methods. The transition states linking the cyclic clusters show high energetic barriers that prevent the spontaneous transformation of the high-energy clusters, $(HNC)_n$, into the low-energy ones, $(HCN)_n$. The effect of the protonation/deprotonation of the linear clusters has also been explored. The results show that $(HNC)_n$ clusters with n values larger than six are thermodynamically more stable as charged systems than as neutral ones. The geometrical results have been analyzed using a Steiner−Limbach plot. The electron density and its Laplacian at the bond critical points correlate with the corresponding bond distances by means of two exponential functions, one for the open shell and another for the closed shell cases.

Introduction

Hydrogen bond (HB) formation induces changes within the monomers that are involved. In many cases, these changes facilitate the aggregation of additional monomers to the initially formed complex. This phenomenon is known as cooperativity. It greatly influences the properties of the monomers and those of the formed clusters. Thus, for instance, the water trimer shows a basicity comparable to ammonia.[1] A number of theoretical studies have been devoted to analyze the cooperativity effects in hydrogen bonded systems.[2]

Linear and cyclic clusters of hydrogen cyanide (HCN) in gas phase have been described in the literature.[3,4,5] The trimer is the smallest cluster that presents both linear and cyclic topologies. Larger linear clusters have been reported in superfluid helium.[6] In the solid state, the configuration adopted by these clusters corresponds to infinite linear chains with intermolecular C···N distances of 3.18 Å.[7]

A number of ab initio studies have been carried out on the $(HCN)_n$ clusters. Thus, in agreement with the experimental data, a similar stability of the linear and cyclic trimers was found using Hartree−Fock (HF) methods.[8] As well, the cooperative effects on the structural, energetic, and spectroscopic properties of linear clusters were studied using HF and MP2 methods.[9,10] The results showed that the nonlinear cooperativity effect could be rationalized in terms of the orbital charge transfer ($lp_N \rightarrow \sigma^*_{CH}$) occurring in the HB. In addition, a detailed analysis of the multiple-body interaction terms of the cooperative effect at the calculated MP2 energies of linear clusters was carried out.[11] A potential function was developed, using over 300 points of the dimer surface, which was able to reproduce the characteristics of the HCN dimer and the two minimum-energy form of the trimer.[12] Moreover, the localized analysis of the HB energies and bond orders in the linear cluster of HCN and HNC was carried out at the DFT level.[13] Finally, the solvation of a proton by protonated clusters of HCN was studied by Meot-Ner[14] and Hirao et al.[15]

The aim of the present article is to focus on the energetic differences of the HCN and hydrogen isocyanide (HNC) clusters and the transition states connecting them. In addition, the effect of the protonation and deprotonation of these clusters has been considered, and the geometrical characteristics of all the complexes have been analyzed using Steiner−Limbach relationships. As well, the electron density properties of the bonds involved in the electron density have been explored within the atoms in molecules (AIM) methodology.

Methods

The geometry of the complexes has been optimized with B3LYP/6-31+G**,[16,17] MP2/6-31+G**,[18] MP2/cc-pVTZ,[19] and MP2/aug-cc-pVTZ computational methods. The minimum or transition state nature of the complexes has been established based on the sign of the harmonic vibrational frequencies calculated at the B3LYP/6-31+G** and MP2/6-31+G** levels using the geometries obtained at the corresponding computational levels.

The interaction energy of the complexes has been calculated as the difference between the total energy of the complexes and those of the isolated monomers. No basis-set superposition error (BSSE) correction has been considered since BSSE corrections may not always improve binding energies of hydrogen-bonded complexes. That is due to the fact that in the counterpoise method[20] a monomer may use the valence and core functions of its partner, which are not available to the monomer in the complex. In general, basis sets that include diffuse functions markedly reduce the effect of BSSE. In addition, it has been shown[21] that uncorrected aug-cc-pVTZ binding energies lie between corrected and uncorrected aug-cc-pVQZ energies.

The electron density of the complexes has been analyzed using AIM methodology[22] with the AIMPAC package.[23]

* To whom correspondence should be addressed. E-mail: marina@unne.edu.ar; ibon@iqm.csic.es. Fax: 34 91 564 48 53.

10.1021/jp052935d CCC: $30.25
Published on Web 08/31/2005

TABLE 1: Interaction Energies (kcal/mol) of Linear and Cyclic Clusters of (HCN) and (HNC)

	linear $(HCN)_n$ clusters				linear $(HNC)_n$ clusters			
	B3LYP/6-31+G*	MP2/6-31+G*	MP2/cc-pVTZ	MP2/aug-cc-pVTZ	B3LYP/6-31+G*	MP2/6-31+G*	MP2/cc-pVTZ	MP2/aug-cc-pVTZ
2	−4.45	−4.90	−4.99	−5.32	−7.00	−7.67	−8.08	−8.39
3	−10.08	−10.84	−11.11	−11.76	−15.92	−17.31	−18.39	−18.95
4	−16.14	−17.13	−17.61	−18.57	−25.90	−27.68	−29.55	−30.34
5	−22.39	−23.56	−24.27		−35.64	−38.38	−41.10	
6	−28.78	−30.06	−31.01	−32.62	−45.86	−49.26	−52.85	−54.06
7	−35.11				−56.21			
8	−41.60	−43.16	−44.61		−67.29	−71.25	−76.65	
9	−48.05				−77.82			
10	−54.51				−88.37			
12	−67.45				−109.53			
	cyclic $(HCN)_n$ clusters				cyclic $(HNC)_n$ clusters			
	B3LYP/6-31+G*	MP2/6-31+G*	MP2/cc-pVTZ	MP2/aug-cc-pVTZ	B3LYP/6-31+G*	MP2/6-31+G*	MP2/cc-pVTZ	MP2/aug-cc-pVTZ
3	−8.43	−10.58	−10.99	−11.79	−9.59	−13.42	−15.06	−15.42
4	−16.32	−18.51	−19.24	−20.39	−22.45	−26.57	−29.71	−30.23
5	−24.22	−26.28	−27.29		−35.69	−39.95	−44.44	
6	−31.79	−33.78	−35.09	−36.90	−48.49	−53.03	−58.68	−59.60
7	−39.14				−60.87			
8	−46.32	−48.26	−50.18		−72.92	−78.28	−85.95	
9	−53.37				−84.71			
10	−60.33				−96.31			
12	−74.06				−119.10			

TABLE 2: Relative Energy of the Cyclic Cluster vs the Corresponding Linear One (kcal/mol)

	$(HCN)_n$				$(HNC)_n$			
cluster size (n)	B3LYP/6-31+G**	MP2/6-31+G**	MP2/cc-pVTZ	MP2/aug-cc-pVTZ	B3LYP/6-31+G**	MP2/6-31+G**	MP2/cc-pVTZ	MP2/aug-cc-pVTZ
3	1.66	0.26	0.12	−0.03	6.33	3.89	3.34	3.53
4	−0.18	−1.38	−1.63	−1.82	3.45	1.11	−0.16	0.11
5	−1.83	−2.72	−3.02		−0.05	−1.57	−3.34	
6	−3.01	−3.72	−4.08	−4.29	−2.63	−3.78	−5.83	−5.54
7	−4.02				−4.66			
8	−4.72	−5.10	−5.57		−5.63	−7.03	−9.30	
9	−5.32				−6.89			
10	−5.83				−7.94			
12	−6.61				−9.57			

Results and Discussion

Neutral Systems. The interaction energies of linear and cyclic clusters of HCN and HNC at the different computational levels are reported in Table 1. The B3LYP/6-31+G** interaction energies, in absolute value, are the smallest of those calculated here. It is significant that as the size of the basis set increases in the MP2 methods, the value of the interaction energy becomes larger, confirming that the use of the BSSE correction does not appear to be necessary. The largest difference observed between the different methods corresponds to the cyclic clusters of HNC where the differences between the B3LYP/6-31+G** and MP2/aug-cc-PVTZ are 37% in the trimer and decrease for larger clusters.

A clear indication of the cooperative effects of these clusters is obtained when the interaction energy is divided by the number of HBs present in the corresponding complex. The variation of this parameter with cluster size has been plotted in Figure 1 for the linear complexes (a similar plot is obtained for the cyclic ones).

Moreover, this simple partition shows that in all the cases, with the exception of the $(HCN)_{12}$ complex, the average HB interaction energy per HB is larger in the linear clusters than in the cyclic ones. As expected, the differences decrease with the cluster size and should be zero for very large clusters. It should be noted that for the same cluster size, the cyclic complexes show one HB more than the linear ones. Thus, the maximum energetic difference that could be expected between a linear and a cyclic cluster should be that corresponding to the average HB interaction energy for that system.

The relative energies of the cyclic vs the linear complexes of $(HCN)_n$ and $(HNC)_n$ are collected in Table 2. The results

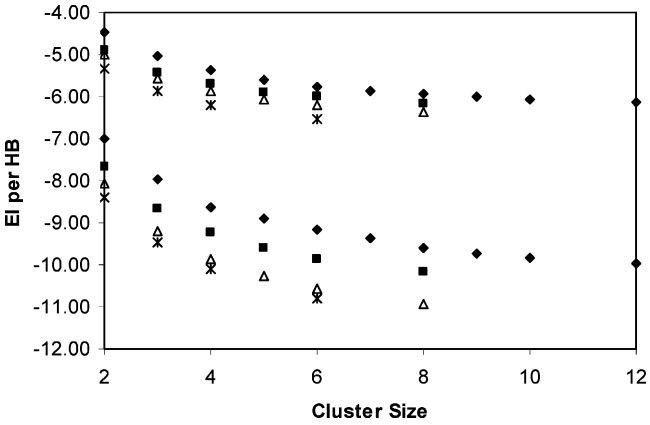

Figure 1. Interaction energy per HB (kcal/mol) for the linear clusters. The upper part corresponds to the $(HCN)_n$ complexes and the lower part to the $(HNC)_n$. Diamonds, squares, triangles, and stars represent the B3LYP/6-31+G**, MP2/6-31+G**, MP2/cc-pVTZ, and MP2/aug-cc-pVTZ results, respectively.

TABLE 3: Fitted Semilogarithmic Equations between the Size of the Cluster, *n*, and the Energy Difference between the Cyclic and the Linear Clusters ($E_{rel} = A^* \ln(n) + B$)

	$(HCN)_n$				$(HNC)_n$			
	B3LYP/6-31+G**	MP2/6-31+G**	MP2/cc-pVTZ	MP2/aug-cc-pVTZ	B3LYP/6-31+G**	MP2/6-31+G**	MP2/cc-pVTZ	MP2/aug-cc-pVTZ
A	−6.084	−5.513	−5.840	−6.131	−11.842	−11.265	−13.050	−13.133
B	8.103	6.251	6.467	6.695	19.166	16.471	17.732	18.087
r^2	0.993	0.998	0.998	1.000	0.991	0.998	0.999	0.998
n.points	9	5	5	3	9	5	5	3

TABLE 4: Geometrical Distances (Å) of the HB in the Cyclic Clusters

cluster size	B3LYP/ 6-31+G**		MP2/ 6-31+G**		MP2/cc-pVTZ		MP2/aug-cc-pVTZ	
$(HCN)_n$	HC	H···N	HC	H···N	HC	H···N	HC	H···N
1	1.070		1.067		1.064		1.065	
3	1.074	2.518	1.069	2.518	1.068	2.438	1.069	2.408
4	1.078	2.271	1.072	2.297	1.072	2.223	1.072	2.203
5	1.080	2.172	1.074	2.218	1.074	2.146		
6	1.082	2.128	1.075	2.181	1.075	2.112	1.076	2.100
7	1.083	2.101						
8	1.083	2.087	1.076	2.150	1.077	2.081		
9	1.084	2.077						
10	1.084	2.069						
12	1.085	2.060						
$(HNC)_n$	HN	H···C	HN	H···C	HN	H···C	HN	H···C
1	1.000		1.000		0.996		0.997	
3	1.010	2.354	1.009	2.329	1.008	2.243	1.010	2.224
4	1.022	2.065	1.018	2.093	1.019	2.025	1.021	2.015
5	1.030	1.964	1.025	2.002	1.027	1.940		
6	1.035	1.919	1.029	1.958	1.032	1.898	1.034	1.894
7	1.039	1.894						
8	1.041	1.878	1.034	1.916	1.038	1.860		
9	1.042	1.868						
10	1.043	1.861						
12	1.045	1.851						

show that for clusters larger than $n = 4$ in the case of HCN complexes and $n = 5$ in the case of HNC ones, the cyclic structures are more stable than the linear ones. Among the methods considered here, B3LYP is the one that tends to stabilize more the linear clusters vs the cyclic ones (more positive values in Table 2). Differences between the different methods tended to converge in the $(HCN)_n$ clusters while the opposite happened in the $(HNC)_n$ ones as the value of *n* increased. Cyclic clusters are more stable for the large clusters of $(HNC)_n$ than in the case of the HCN. A semilogarithmic relationship ($E_{rel} = A^* \ln(n) + B$) nicely fits the relative energies, E_{rel}, with the cluster size, *n*, as shown in Table 3. The absolute value of the parameter *A* provides an idea on how the differences will increase with larger clusters.

Analysis of the geometries of the different clusters shows that the cooperativity effects produce a shortening of the distance between the hydrogen atom and the electron donor atom and a lengthening of the covalent bond in the electron acceptor moiety as can be seen in the results reported in Table 4 for the cyclic clusters. In the case of the linear clusters, the geometrical effects are more pronounced in the middle of the chains monomers. The shortest distance obtained for the heavy atoms involved in the HB is 3.13 Å for the linear $(HCN)_{12}$ cluster calculated at the B3LYP/6-31+G** level. This result closely resembles the experimental findings for the crystal structure of an infinite HCN chain (3.18 Å).[7]

The formation of HB complexes has been associated to a charge transfer and a subsequent increment of the dipole moment when compared to the isolated monomers. The results obtained for the average dipole moment enhancement per molecule of the linear cluster are shown in Table 5. The results show that in the $(HNC)_n$ clusters the enhancement is twice that of the corresponding $(HCN)_n$ ones, in agreement with the interaction energies obtained for them. The large increment of the dipole moment enhancement in the smaller clusters tends to slow in the larger ones, but still for the cluster with 12 units an increment of a 4% is observed when compared to that of 10 units.

Transition States Corresponding to the Transformation of the Cyclic Clusters. A multiple proton transfer within the cyclic clusters should convert the $(HNC)_n$ clusters into the $(HCN)_n$ ones and vice versa. Even though a large energy gap is observed between these two clusters, specially for large *n* values, no spontaneous conversion from the least to the most stable one is observed. The initial attempts to locate the simultaneous proton transfer from all the molecules in a given cluster provided structures with more than a single imaginary frequency with the exception of the trimer at the B3LYP/6-31+G** level. In general, the transition state (TS) structures are highly asymmetric (as an example the case for the hexamer is illustrated in Figure 2) since once a hydrogen atom is transferred, the simultaneous transfer of the rest of the hydrogen atoms toward the $(HCN)_n$ cluster takes place.

The calculated barriers for the TS using the $(HNC)_n$ cluster as a starting point are represented in Figure 3. The values obtained at the MP2/cc-pVTZ level are about 4 kcal/mol lower than those of the B3LYP/6-31+G** and MP2/6-31+G** computations. In all the cases, a rapid attenuation of the energy

TABLE 5: Average Dipole Moment Enhancement per Molecule in the Linear Clusters (debye)

	$(HCN)_n$				$(HNC)_n$			
cluster size	B3LYP/6-31+G**	MP2/6-31+G**	MP2/cc-pVTZ	MP2/Aug-cc-pVTZ	B3LYP/6-31+G**	MP2/6-31+G**	MP2/cc-pVTZ	MP2/Aug-cc-pVTZ
1	0.00	0.00	0.00	0.00	0.00	0.00	0.00	0.00
2	0.43	0.37	0.41	0.40	0.63	0.60	0.63	0.62
3	0.66	0.57	0.63	0.62	1.00	0.93	1.00	0.99
4	0.81	0.68	0.76	0.75	1.23	1.15	1.24	1.23
5	0.90	0.76	0.85	0.84	1.40	1.31	1.41	1.39
6	0.97	0.81	0.91	0.90	1.52	1.42	1.53	1.51
7	1.02				1.61			
8	1.06	0.89			1.68	1.57		
9	1.09				1.74			
10	1.12				1.79			
12	1.16				1.86			

Figure 2. Geometry of the cyclic clusters of $(HNC)_6$ and $(HCN)_6$ and the corresponding transition state.

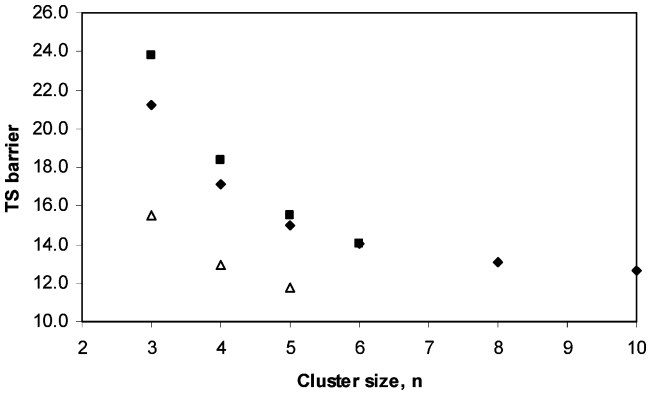

Figure 3. Calculated barrier (kcal/mol) of the TS of the proton transfer in the cyclic clusters (the $(HNC)_n$ cluster is used as reference). Diamonds, squares, and triangles represent the B3LYP/6-31+G**, MP2/6-31+G**, and MP2/cc-pVTZ, respectively

TABLE 6: Average Distance (Å) of the Heavy Atoms to the Center of the Ring in the Minima and TS Structures Calculated at the B3LYP/6-31+G Level**

cluster size	$(HCN)_n$	$(HNC)_n$	TS
3	2.255	2.193	1.887
4	2.868	2.736	2.485
5	3.515	3.337	3.114
6	4.177	3.958	3.741
8	5.516	5.219	5.015
10	6.866	6.491	6.293

is obtained with the size of the cluster, thus the results at the B3LYP/6-31+G** level with $n = 8$ only differ by 0.4 kcal/mol from those at $n = 10$.

Geometrically the TS structure is compressed when compared to the $(HNC)_n$ and $(HCN)_n$ cyclic structures as can be seen from the average values of distance of the center of the ring and the heavy atoms obtained for the minima and TS structures (see Table 6). In the cases studied, the contraction corresponds to an average of 0.2 Å of the whole cycle toward its center when compared to the $(HNC)_n$ structures. This contraction has been described in other proton-transfer processes.[24−26] Furthermore, the TS structure more closely resembles the highest energy minima, in this case the $(HNC)_n$ clyclic cluster, in agreement with the Hammond postulate.

A perfect linear relationship has been found between this average distance of the heavy atoms to the center of the ring and the number of monomers in the cluster or TS structures (square correlation coefficients, R^2, of 1.000 for the HCN and HNC cluster and 0.999 for the TS structures). These results indicate that the mentioned average distance parameter can be used as a measure of the cluster size.

Acidity and Basicity of the Neutral Clusters. The protonation or deprotonation of the clusters presents a linear disposition with a reordering of the hydrogen atoms to obtain the maximum number of HCN molecules, on one hand, and to solvate the charged species, on the other. Thus the resulting species can be schematically represented as $[HNC\cdots HNCH\cdots(NCH)_{n-2}]^+$ for the cations and $[CNH\cdots CN\cdots(HCN)_{n-2}]^-$ for the anions, independently of the starting point $(HCN)_n$ or $(HNC)_n$. This reordering increases significantly the apparent acidity and proton affinity of the $(HNC)_n$ clusters when compared to the monomers (Table 7).

The experimental values for the proton affinity of the monomers (170.4 and 184.6 kcal/mol for HCN and HNC, respectively) as well as the enthalpic contribution to the acidity of the HCN system (350.90 ± 0.20) are nicely reproduced in all the calculations reported here.

It is important to notice that for $(HNC)_n$ with $n \geq 5$ (6 at the B3LYP/6-31+G** level) the PA is larger than the acidity which indicates that the autoionization of the two clusters is energetically favorable.

The HB distance is very short in the monomers surrounding the charged species, and it gradually increases as the number of intermediate molecules increases. The distance between the heavy atoms (Table 8) is always shorter in the charged species than in the $(HCN)_n$ cluster due to the shortening of the HB distance previously mentioned. In the case of the $(HNC)_n$ clusters, the protonation/deprotonation produces a spontaneous generation of HCN molecules. Since the HCN molecules present larger HB distances, the shortening due to the presence of charged molecules is compensated.

General Analysis. Two aspects have been considered together for all the stationary structures, minima and TS, calculated so far, the geometry, and the electron density around the hydrogen bond. The geometry of the complexes has been analyzed using the bond valence model proposed by Pauling. In this model, the total valence of the hydrogen atom within a HB (Scheme 1) should be equal to 1 (eq 1). The r_{01} and r_{02} parameters represent the bond distance for the isolated systems while b is an adjustable parameter that in general has an approximate value of 0.4. A reformulation of eq 1 provides the Steiner−Limbach relationship (eq 2), [27−29] where the distance between the heavy atoms involved in the HB $(r_1 + r_2)$ is related to the relative position of the hydrogen atom $(r_1 - r_2)$. The geometry of the minima and TS of the complexes for all the HBs calculated at the B3LYP/6-31+G** level (254 cases) have been plotted in Figure 4. The shape of the curve indicates that the proton-transfer process ($r_1 - r_2$ values near to zero) proceeds with a compression of the system (small values of $r_1 + r_2$), and clearly it can be seen that the values obtained here fit very well the Steiner−Limbach relationship

$$e^{(r_{01}-r_1)/b} + e^{(r_{02}-r_2)/b} = 1 \quad (1)$$

$$(r_1 + r_2) = 2r_{02} + (r_1 - r_2) + 2b \ln(1 + e^{(r_{01}-r_{02}-r_1+r_2)/b}) \quad (2)$$

The large number of HBs considered and their distribution from covalent to weakly bonded HBs allow us to study the

TABLE 7: Acidity and Proton Affinity of the Clusters (kcal/mol)[a]

	acidity				proton affinity			
$(HCN)_n$	B3LYP/6-31+G**	MP2/6-31+G**	MP2/cc-pVTZ	MP2/aug-cc-pVTZ	B3LYP/6-31+G**	MP2/6-31+G**	MP2/cc-pVTZ	MP2/aug-cc-pVTZ
1	347.45	349.67	356.70	355.59	167.92	167.07	167.82	173.92
2	329.23	333.74	337.38	338.60	186.55	183.21	185.01	191.01
3	322.24	330.89	331.36	334.99	194.28	189.54	191.75	196.94
4	317.66	327.09	327.18	330.69	198.05	191.78	194.21	199.69
5	315.47	325.33	325.23	328.65	199.93	191.77	194.96	200.36
6	314.12	324.16	323.97	327.31	201.21	192.86	196.14	201.61
7	313.32				201.97			
8	312.82	323.08	322.80		202.44	193.88	197.23	
9	312.45				202.81			
10	312.16				203.08			
$(HNC)_n$	B3LYP/6-31+G**	MP2/6-31+G**	MP2/cc-pVTZ	MP2/aug-cc-pVTZ	B3LYP/6-31+G**	MP2/6-31+G**	MP2/cc-pVTZ	MP2/aug-cc-pVTZ
1	334.41	331.80	339.12	337.74	180.96	184.94	185.40	191.77
2	304.91	300.00	304.52	305.97	210.88	216.95	217.88	223.64
3	287.46	282.27	284.39	288.63	229.06	238.16	238.72	243.30
4	273.21	264.13	266.73	271.05	242.51	254.74	254.66	259.33
5	260.80	248.11	251.42	255.94	254.60	268.99	268.77	273.07
6	249.55	232.76	236.89	241.64	265.79	284.27	283.22	287.27
7	239.06				276.23			
8	229.73	203.80	209.71		285.53	313.15	310.33	
9	219.84				295.42			
10	210.04				305.20			

[a] The neutral linear clusters have been used as reference.

TABLE 8: Distance between the Extreme Heavy Atoms (Å) in the Neutral and Charged Linear Clusters Calculated at the B3LYP/6-31+G Level**

cluster size	$(HCN)_n$	$(HNC)_n$	protonated system	deprotonated system
1	1.158	1.176	1.140	1.184
2	5.604	5.410	5.057	5.197
3	9.944	9.535	9.132	9.207
4	14.254	13.626	13.233	13.412
5	18.550	17.694	17.460	17.641
6	22.841	21.756	21.709	21.892
7	27.128	25.810	25.971	26.154
8	31.417	29.859	30.237	30.422
9	35.698	33.907	34.508	34.691
10	39.980	37.953	38.781	38.964

SCHEME 1: Definition of r_1 and r_2

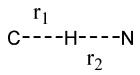

evolution of the electron density parameters at the bond critical points for the CH and NH bonds. The results for the electron density, ρ_{BCP}, and its Laplacian, $\nabla^2\rho_{BCP}$, at the bond critical point are shown for the NH bonds in Figure 5 (results for the CH bonds are similar to those shown in Figure 5). The ρ_{BCP} has been correlated with interatomic distances exponentially using two different functions, one for the closed shell interactions and another for the open shell ones.[30] These two exponential functions can be integrated in a unique equation using a joint function as described previously.[30]

The Laplacian shows a negative value for the open shell interactions and presents a small maximum in the positive region that corresponds to closed shell bonds. A similar behavior has been already described for the F···H interaction ranging from weak interactions to covalent bonds.[30]

Conclusions

A theoretical study of linear and cyclic clusters of HCN and HNC has been carried out using DFT and MP2 ab initio levels. The results show that cyclic clusters are more stable than linear ones in those cases where the number of monomers considered is larger than four. The effect of the cooperativity in those clusters has been illustrated by the reduction of the HB length, increment of the interaction energy, and the dipole moment per HB.

The transition states that link the cyclic $(HNC)_n$ and $(HCN)_n$ clusters show a significant barrier, even when the value of n is large, which corresponds to very large energetic differences between the two clusters. The structures of the TS are very asynchronous, and in general, the transfer of a single hydrogen atom from the $(HNC)_n$ cluster evolves to a complete transformation of the system toward $(HCN)_n$ without any additional barrier.

The protonation/deprotonation of the linear clusters produce a reordering of the hydrogen atoms, yielding structures with a

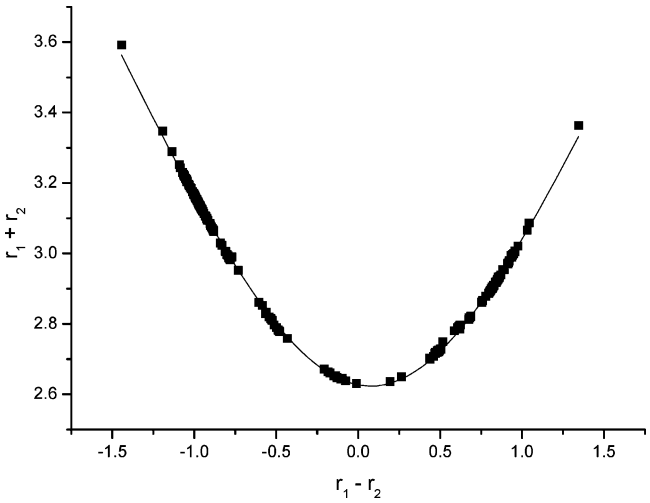

Figure 4. Steiner−Limbach correlation of the geometrical parameters for all minima and TS structures calculated here at the B3LYP/6-31++G** computational level. The fitted curve corresponds to eq 2 and to the following adjusted parameters: $r_{01} = 1.04654 \pm 0.0006$, $r_{02} = 0.9708 \pm 0.0009$, $b = 0.437 \pm 0.002$, and the square correlation efficient, $r^2 = 0.999$, for a total number of points, $n = 254$.

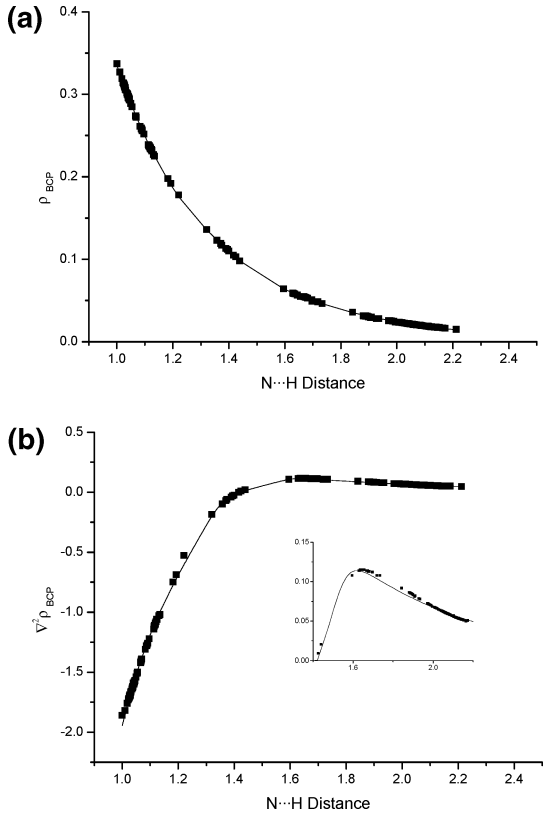

Figure 5. Electron density (a) and Laplacian of the electron density (b) at the bond critical point vs the N···H distance (Å). The positive region in the Laplacian plot is shown in detail. The points have been fitted using a joint function composed of two exponential equations as described in ref 30. The square correlation coefficients obtained for the fitted curves are 0.99998 and 0.9998 for the electron density and the Laplacian, respectively, and the number of points considered are 253 in both cases.

larger number of HCN molecules that simultaneously "solvate" the charged species. This process results in a large acidity and proton affinity of the $(HNC)_n$ clusters. For those cases with n values larger than 5, the sum of the energies of the protonated and deprotonated systems is lower than the corresponding energies of the isolated clusters of the same size.

The geometric results of all the minima and TS calculated here have been conveniently fitted to a Steiner−Limbach plot. This plot shows the dependency of the relative position of the hydrogen atom in a HB systems with the distances between the hydrogen and the two heavy atoms involved in the interaction. Finally, the values of the electron density and the Laplacian at the bond critical points have been fitted with a joint function that includes two exponential equations. One of the exponential equations covers the open shell regime whereas the other deals with the closed shell one.

Acknowledgment. I.A. and J.E. thank the Ministerio de Ciencia y Tecnología of Spain for financial support (Project No. BQU-2003-01251). Thanks are given to the CTI (CSIC) and CESGA for allocation of computer time. M.S., P.F.P. and G.A.A. acknowledge financial support from CONICET, ANPCyT and SGCyT-UNNE (PI-651). M.S. wants to thank the support of the Intituto de Química Médica during her visit to this institution.

References and Notes

(1) Mohr, M.; Marx, D.; Parinello, M.; Zipse, H.; *Chem. −Eur. J.* **2000**, *6*, 4009. Mohr, M.; Zipse, H. *Phys. Chem. Chem. Phys.* **2001**, *3*, 1246.
(2) Scheiner, S. *Hydrogen Bonding. A theoretical perspective*; Oxford University Press: Oxford, U.K., 1997 and therein cited references.
(3) Jucks, K. W.; Miller, R. E. *J. Chem. Phys.* **1988**, *88*, 6059.
(4) Ruoff, R. S.; Emilsson, T.; Klots, T. D.; Chuang, C.; Gutowsky, H. S. *J. Chem. Phys.* **1988**, *89*, 138.
(5) Jucks, K. W.; Miller, R. E. *J. Chem. Phys.* **1988**, *88*, 2196.
(6) Nauta, K.; Miller, R. E. *Science* **1999**, *283*, 1895.
(7) Dulmage, W. J.; Lipscomb, W. N. *Acta Crystallogr.* **1951**, *4*, 330.
(8) Kurning, I. J.; Lischka, H.; Karpfen, A. *J. Chem. Phys.* **1990**, *92*, 2469.
(9) King, B. F.; Weinhold, F. *J. Chem. Phys.* **1995**, *103*, 333.
(10) King, B. F.; Farrar, T. C.; Weinhold, F. *J. Chem. Phys.* **1995**, *103*, 348.
(11) Rivelino, R.; Chaudhuri, P.; Canuto, S. *J. Chem. Phys.* **2003**, *118*, 10593.
(12) Cabaleiro-Lago, E. M.; Ríos, M. A. *J. Chem. Phys.* **1998**, *109*, 3598.
(13) Chen, C.; Liu, M. H.; Wu, L. S. *THEOCHEM* **2003**, *630*, 187.
(14) Met-Ner (Mautner), M. *J. Am. Chem. Soc.* **1978**, *100*, 4694.
(15) Hirao, K.; Yamabe, S.; Sano, M, *J. Phys. Chem.* **1982**, *86*, 2626.
(16) Becke, A. D. *J. Chem. Phys.* **1993**, *98*, 5648. Lee, C.; Yang, W.; Parr, R. G. *Phys. Rev. B* **1988**, *37*, 785.
(17) Hariharan, P. A.; Pople, J. A. *Theor. Chim. Acta* **197**3, *28*, 213.
(18) Møller, C.; Plesset, M. S. *Phys. Rev.* **1934**, *46*, 618.
(19) Dunning, T. H., Jr. *J. Chem. Phys.* **1989**, *90*, 1007.
(20) Boys, S. F.; Bernardi, F. *Mol. Phys.* **1970**, *19*, 553.
(21) Del Bene, J. E.; Shavitt, I. in *Molecular Interactions: From van der Waals to Strongly Bound Complexes*; Scheiner, S. J., Ed.; John Wiley & Sons: Sussex, U.K., 1997; pp 157−179.
(22) Bader, R. F. W. *Atoms in Molecules: A Quantum Theory*; The International Series of Monographs of Chemistry; Halpen, J., Green, M. L. H., Eds.; Clarendon Press: Oxford, U.K., 1990.
(23) Bieger-Konig, F. W.; Bader, R. F. W.; Tang, T. H. *J. Comput. Chem.* **1982**, *3*, 317.
(24) De Paz, J. L. G.; Elguero, J.; Foces-Foces, C.; Llamas-Saiz, A. L.; Aguilar-Parrilla, F.; Klein, O.; Limbach, H. H. *J. Chem. Soc., Perkin Trans. 2* **1997**, 101.
(25) Picazo, O.; Alkorta, I.; Elguero, J. *J. Org. Chem.* **2002,** *67*, 1515.
(26) Picazo, O.; Alkorta, I.; Elguero, J., Yañez, M.; Mo, O. *J. Phys. Org. Chem.* **2005**, *18*, 491.
(27) Steiner, Th.; Saenger, W. *Acta Crystallogr., Sect. B* **1994**, *B50*, 348. Steiner, Th. *Chem. Commun.* **1995**, 1331.
(28) Ramos, M.; Alkorta, I.; Elguero, J.; Golubev, N. S.; Denisov, G. S.; Benedict, H.; Limbach, H.-H. *J. Phys. Chem. A* **1997**, *101*, 9791.
(29) Brown, I. D. *Acta Crystallogr., Sect. B* **1992**, *B48*, 553.
(30) Espinosa, E.; Alkorta, I.; Elguero, J.; Molins, E. *J. Chem. Phys.* **2001**, *117*, 5529.